Chinese Chemical Letters 36 (2025) 109734

Contents lists available at ScienceDirect

Chinese Chemical Letters

journal homepage: www.elsevier.com/locate/cclet

Fisetin micelles precisely exhibit a radiosensitization effect by inhibiting PDGFRβ/STAT1/STAT3/Bcl-2 signaling pathway in tumor

Yuanyuan Zeng[a,1], Fang Liu[b,1], Jun Wang[a,1], Bianfei Shao[c], Tao He[d], Zhongzheng Xiang[a], Yan Wang[e], Shunyao Zhu[f], Tian Yang[a], Siting Yu[a], Changyang Gong[d], Lei Liu[a,*]

[a] Department of Radiation Oncology, Cancer Center, State Key Laboratory of Biotherapy, West China Hospital, Sichuan University, Chengdu 610041, China
[b] Department of Radiation Oncology, The Affiliated Cancer Hospital of Zhengzhou University, Henan Cancer Hospital, Zhengzhou 450000, China
[c] Chongqing Key Laboratory of translational Research for Cancer Metastasis and individualized Treatment, Chongqing University Cancer Hospital, Chongqing 400030, China
[d] Department of Biotherapy, Cancer Center and State Key Laboratory of Biotherapy, West China Hospital, Sichuan University, Chengdu 610041, China
[e] Department of Pharmacy, The First Affiliated Hospital of Wannan Medical College, Yijishan Hospital of Wannan Medical College, Wuhu 241004, China
[f] Institute of Surgery Research, Daping Hospital, Third Military Medical University, Chongqing 400042, China

ARTICLE INFO

Article history:
Received 16 January 2024
Revised 22 February 2024
Accepted 25 February 2024
Available online 8 March 2024

Keywords:
Fisetin
Polymetric micelles
Radiotherapy
Radiosensitizer
Platelet-derived growth factor receptor-β

ABSTRACT

It is of great significance to find safe and effective radiosensitizers. A primary investigation has been made on fisetin's modification of radiation effect, but its radiosensitization and related mechanisms still need to be deeply clarified. Furthermore, fisetin with high hydrophobicity is difficult to dissolve in water, severely limiting its research and application. In this study, we fabricated a safe and soluble radiosensitizer fisetin micelle for precisely enhancing radiotherapy by inhibiting platelet-derived growth factor receptor-β (PDGFRβ)/signal transducer and activator of transcription 1 (STAT1)/signal transducer and activator of transcription 3 (STAT3)/B cell lymphoma 2 (Bcl-2) signaling pathway in the tumor. Systematic and detailed studies were performed to verify its radiosensitization effect *in vitro* and *in vivo*. On the cellular level, fisetin micelles selectively increased the radiosensitivity of tumor cells (CT26 and 4T1 cells) and had little effect on the sensitivity of normal mouse cells (L929 cells) to radiation. In the mouse models of colon and breast cancers, fisetin micelles showed an efficient radiosensitization capacity without apparent toxicity. Additionally, we first found that fisetin micelles played a radiotherapy sensitization role by inhibiting the PDGFRβ/STAT1/STAT3/Bcl-2 pathway activity. In general, this work not only confirmed that fisetin micelles precisely exhibit a radiosensitization effect *in vitro* and *in vivo*, but also profoundly explored its mechanisms underlying, to provide a theoretical and experimental basis for the clinical application of fisetin micelles.

Radiotherapy, which employs high-energy rays to kill cancer cells with no depth restriction, is one of the most common and effective treatments for cancer therapy. Almost 60% of cancer patients require radiotherapy intervention during treatment [1]. Unfortunately, tumors are mostly not sensitive to radiation and require high doses of radiotherapy to kill tumor cells effectively, which leads to healthy tissue damage and exceeds patients' tolerance [2]. Radiosensitizers are chemicals or drugs that can strengthen the biological effects of radiation, to achieve better clinical efficacy under the same radiation dose or protect normal tissues with a lower radiation dose while obtaining the same therapeutic effect [3]. At present, the most widely used radiosensitizers in clinical practice have still focused on conventional chemotherapeutic agents, such as cisplatin and paclitaxel [4,5]. However, traditional radiosensitizers still face some insurmountable challenges in clinical practice. A significant challenge is the drug side effects such as renal and hematological toxicity caused by small molecular chemotherapeutic drugs after intravenous injection [6–9]. Another problem is that most chemotherapy drugs could easily form an essentially irreversible complex with plasma albumin to lead limited radiosensitization activity [10]. Thus, the development of drugs and methods to improve the therapeutic index of radiosensitization has been a significant research objective.

With the development of nanomedicine, nanoparticle (NP) formulations of drugs offer an unprecedented opportunity for radiosensitizers [11–14]. Compared with traditional medications,

* Corresponding author.
E-mail address: liuleihx@gmail.com (L. Liu).
[1] These authors contributed equally to this work.

https://doi.org/10.1016/j.cclet.2024.109734
1001-8417/

nanoparticles possess unique characteristics suited for the enhancement of radiation therapy [12,15,16]. During recent decades, a number of different radiosensitizers, many of which are nanoparticles containing small molecule chemotherapeutics, have been widely explored to enhance the therapeutic efficiency and specificity of radiotherapy [17–19]. In addition, nanoparticles containing high Z-elements capable of absorbing ionizing radiation, have been investigated for radiosensitizers in clinical trials, such as AGuIX (Gd-based) and NBTXR3 (Hf-based) [20]. Unfortunately, radiosensitizers containing high Z-elements also have obvious shortcomings. The non-biodegradation of metals and long-term accumulation in the body, cause biosafety concerns and could limit their use in radiotherapy treatment [21]. Therefore, safe and biodegradable drugs to strengthen radiosensitization deserve further investigation.

There has been increasing attention on anti-tumor drugs from natural products, especially plants [22]. A series of findings validate that flavonoids can potentially kill tumor cells and enhance the efficacy of radiotherapy, such as flavopiridol and apigenin [23,24]. Fisetin, 3,3′,4′,7-tetrahydroxyflavone, is a hydrophobic plant extract widely distributed in vegetables and fruits, and belongs to the dietary flavonoids that exert numerous biological activities [25]. A primary investigation *in vitro* showed that fisetin exhibited a radiosensitizing impact in colorectal cancer cells [26]. Meanwhile, previous studies have reported that fisetin exerts antiinflammatory, hepatoprotective, neurotrophic, and neuroprotective effects [25]. which makes it possible to develop fisetin as a novel radiosensitizer with high safety. Nevertheless, fisetin has high hydrophobicity and low oral bioavailability, severely limiting its animal pharmacological research and clinical applications [27]. Studies on the influence of fisetin on radioresponse of tumors *in vivo* are scarce, and detailed molecular mechanisms had not been fully investigated [26]. Thus, to prove its radiosensitization effect and underlying mechanisms for future development, the problems of poor dispersibility and low bioavailability of fisetin need to be resolved.

Herein, we fabricated fisetin-loaded polymeric micelles with good dispersibility, achieving a precise and effective radiotherapy sensitization for tumors. As evidenced by colony-forming assay and sensitization enhancement ratios (SERs) on tumor cells (CT26 cells and 4T1 cells) and normal tissue cells (L929 cells), we found that fisetin micelles precisely enhanced the *in vitro* tumor cells killing efficacy induced by X-ray irradiation. Afterward, the main ways that functioned in radiation sensitivity were investigated. Detailed mechanism studies demonstrated that fisetin micelles could exert a radiosensitization effect by increasing intracellular levels of reactive oxygen species (ROS), inhibiting radiation damage repair, inducing cell cycle arrest, and tumor cell apoptosis. Interestingly, we found that fisetin micelles could inhibit the activity of the platelet-derived growth factor receptor-β (PDGFRβ)/signal transducer and activator of transcription 1 (STAT1)/signal transducer and activator of transcription 3 (STAT3)/B cell lymphoma 2 (Bcl-2) pathway to play the role of radiotherapy sensitization. Lastly, enhancement factor (EF) values verified the radiosensitization effect of fisetin micelles in both CT26 and 4T1 tumor models. Importantly, no appreciable toxicity to mice was detected using blood chemistry analysis and careful histological examination after i.v. injection of fisetin micelles. Consequently, this work did not only confirm the radiosensitization effect of fisetin-loaded polymeric micelles and quantify the capability *in vitro* and *in vivo*, but also profoundly explored the molecular mechanisms of fisetin-loaded polymeric micelles for enhanced radiotherapy sensitization, hoping to pave the way for a better understanding of its radiosensitization mechanism and be a reference for promoting its clinical translation possibilities.

In this study, fisetin was loaded into the monomethyl poly(ethylene glycol)-poly(ε-caprolactone)-poly(trimethylene carbonate) (MPEG-P (CL-*ran*-TMC)) micelles using a thin-film dispersion method without any surfactants or additives. TMC and ε-caprolactone (ε-CL) were used as hydrophobic blocks to form the core of the micelles that encapsulated fisetin, while the hydrophilic segment MPEG surrounded this core as an outer shell, effectively preventing the attack of the biological system. As ascertained by ^{1}H NMR (Fig. 1A), MPEG-P(CL-*ran*-TMC) polymer was successfully synthesized, with a molecular weight of 4416 (PEG/PCL/TMC: 2000/1837/579). The ultraviolet–visible (UV–vis) wavelength-scanning spectrums (Fig. 1B) showed that both free fisetin and fisetin micelles had an absorption peak at 367 nm, while blank micelles had no prominent absorption peak, indicating that fisetin was successfully loaded into the polymeric micelles. It was determined that the best ratio of fisetin and polymer micelles was 5:95 (w/w) after comparing the parameters of a series of different dosage ratios of fisetin micelles (Table S1 in Supporting information). Compared with free fisetin, fisetin micelles had good dispersibility in water and formed yellow, homogeneous transparent solution (Fig. 1C). The transmission electron microscopy (TEM) image revealed the spherical shape of fisetin micelles in aqueous solution (Fig. 1D). The prepared fisetin micelles (5:95) were characterized with small particle size (30 ± 1 nm, Fig. 1E), uniform distribution (polydispersity index (PDI) 0.14 ± 0.02), and were negatively charged (zeta potential -6.09 ± 4.27 mV, Fig. S1 in Supporting information). The diameter observed by TEM was consistent with the analysis by dynamic light scattering (DLS), demonstrating that fisetin micelles were well-dispersed in aqueous solution. Meanwhile, fisetin micelles exhibited good stability in aqueous solutions, with no significant changes in size observed over a period of 7 days (Fig. 1F), and remaining yellow, homogeneous transparent solution after 7 days from the initial preparation (Fig. 1C). Moreover, the efficient encapsulation (EE) and drug loading (DL) of the fisetin micelles were 92.49% ± 0.62% and 4.62% ± 0.03%, respectively. These results indicated that prepared fisetin micelles, characterized by small particle size, uniform distribution, and high encapsulation efficiency, demonstrated excellent dispersibility and stability in water, enabling intravenous injection.

Then, the drug release behaviors of free fisetin and fisetin micelles were evaluated. As indicated in Fig. 1G, the release of fisetin from the free fisetin group was more than 50% at 1 h, markedly decreased from the fisetin micelles group (12.60% ± 0.71%). In the first 6 h, approximately 80% of fisetin was released into the outside media in the free fisetin group, compared with only 39% in the fisetin micelles group. The high *in vitro* release rate of fisetin in fisetin micelles might be attributed to the hydrogen bonding between the hydrophobic core and fisetin, effectively delaying the release of fisetin [28]. This contributes to improving the safety of the drug while maintaining an effective and stable blood concentration. In addition, regardless of the time point of 2 and 4 h, intracellular fisetin cumulant in fisetin micelles group was significantly more than in the free fisetin group (Figs. 1H and I and Fig. S2 in Supporting information), demonstrating that encapsulation of fisetin into polymeric micelles enhances the cellular delivery of fisetin.

Before the evaluation of radiosensitization effect, blank micelles, free fisetin and fisetin micelles were separately incubated with tumor cells (CT26 and 4T1 cells) and normal cells (L929 cells) to verify their cytotoxicity. As indicated in Fig. S3 (Supporting information), blank micelles showed no obvious effect on viability of tumor cells and normal cells, even at a high concentration, suggesting that MPEG-P(CL-*ran*-TMC) copolymer could be safely used as a drug delivery carrier. However, free fisetin and fisetin micelles inhibited cell viabilities in a dose and time-dependent manner (Fig. S4 in Supporting information). For CT26, 4T1 and L929 cells, the half-maximal inhibitory concentration (IC_{50}) values of fisetin micelles were lower than those of free fisetin for 24 h (26.78 *vs.* 104.89 μg/mL, 30.21 *vs.* 36.01 μg/mL, and 42.60 *vs.* 107.34 μg/mL, re-

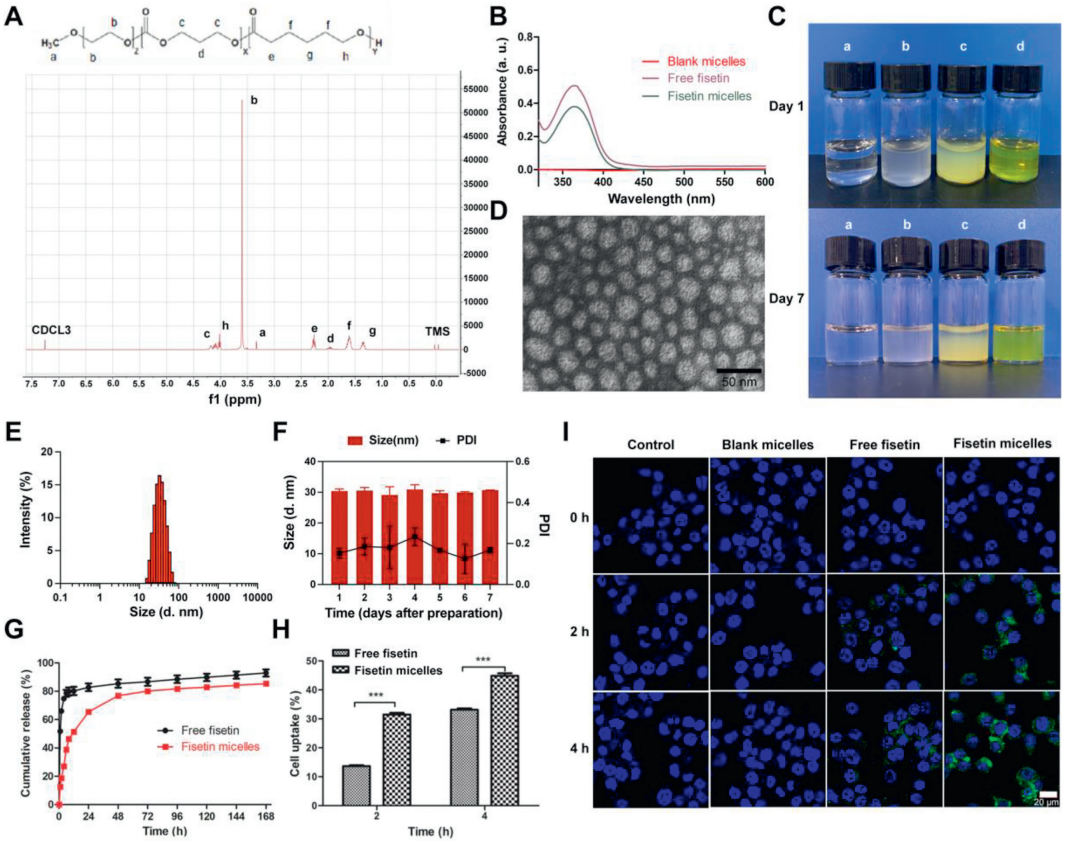

Fig. 1. Characterization of fisetin micelles. (A) ^{1}H NMR spectrum of MPEG-P (CL-*ran*-TMC) copolymer. (B) UV–vis absorption spectrums of blank micelles, free fisetin and fisetin micelles. (C) Appearance of normal saline (a), blank micelles (b), free fisetin (c) and fisetin micelles (d) on day 1 and 7 after preparation. (D) TEM image of fisetin micelles. (E) Size distribution of fisetin micelles. (F) Diameter size and PDI of fisetin micelles dispersed in water for 7 days. (G) Drug release behaviors of free fisetin and fisetin micelles. (H) Intracellular uptake rates of fisetin accumulated in CT26 cells. (I) Fluorescent images of CT26 cells treated with medium, blank micelles, free fisetin and fisetin micelles under a confocal microscope. The nuclei were stained blue with 4′,6-diamidino-2-phenylindole (DAPI) and the cellular distribution of fisetin was shown as green fluorescence in the cytosol. Scale bar: 20 μm. Data are presented as the means ± standard deviation (SD) ($n = 3$). $^{***}P < 0.001$.

spectively) and 48 h (15.72 *vs.* 35.33 μg/mL, 9.77 *vs.* 12.51 μg/mL, and 36.89 *vs.* 96.58 μg/mL, respectively). From this, the cell viability inhibition effect of fisetin micelles was stronger than that of free fisetin at the same concentration, which may contribute to the higher cellular uptake of fisetin micelles. Besides, 30% inhibitory concentration (IC_{30}) values of fisetin for 24 h were 17.26 μg/mL for CT26 cells, 4.59 μg/mL for 4T1 cells and 17.06 μg/mL for L929 cells. Regarding IC_{30} values, the intervention concentrations of fisetin were chosen (15 μg/mL for CT26 and L929 cells, 5 μg/mL for 4T1 cells).

Subsequently, the radiosensitization effect of fisetin micelles was explored by fitting cell survival curves and calculating radiobiological parameters with multi-target/single-hit model. SER was expressed as mean lethal dose (D0) of the radiotherapy alone group/D0 of the combined treatment group. 4T1 cells, widely used to establish triple-negative breast cancer (TNBC) mouse model, were highly invasive and insensitive to radiotherapy [29], which was consistent with our research findings. As shown in Figs. 2A and B and Table S2 (Supporting information), the CT26 cells demonstrated a moderate level of radiosensitivity, with a D0 value of 2.09 Gy, whereas the 4T1 cells exhibited radioresistance, with a higher D0 value of 4.22 Gy. Though fisetin micelles were not as effective in sensitizing 4T1 cells as CT26 cells (SER of 1.6 for 4T1 and 2.3 for CT 26 cells), we demonstrated that fisetin micelles had a stronger radiosensitization effect than free fisetin (SER of 1.6 *vs.* 1.51 for 4T1). Importantly, comparing the SERs of fisetin micelles in tumor cells and normal cells, we found fisetin micelles sensitized tumor cells (SERs of 2.3 for CT26 and 1.6 for 4T1 cells) to radiation precisely, while had little effect on the sensitivity of mouse normal cells (SER of 1.19 for L929 cells, Fig. S5 and Table S2 in Supporting information), making its clinical application possible.

Besides, the survival of tumor cells following irradiation depends on the balance of radiation damage and repair. On the one hand, radiation-induced ROS interaction with cellular contents is an essential mechanism of radiation damage to cells [30]. As can be seen in Figs. 2C and D, ROS accumulated in cells pretreated with fisetin micelles for 24 h were significantly higher than those in other groups. On the other hand, DNA is the primary target for radiation-induced cell killing, and DNA double-strand breaks are thought to be the main lethal events, while DNA damage repair capacity is negatively correlated with cell radiosensitivity. As illustrated in Figs. 2E and F, when a single dose of 6 Gy was split equally into two or three doses (3/3 Gy and 2/2/2 Gy) administered several hours apart, cell surviving fractions increased (the repair rates were 1.43 and 1.62, respectively) due to the repair of sublethal damage (mainly DNA single strand breaks) [31]. However, the repair rates were significantly reduced after fisetin micelles pretreatment, which were 1.00 and 1.11 after 3/3 Gy and 2/2/2 Gy fractional radiotherapy, respectively. Fisetin micelles inhibited the repair of radiation-induced sublethal damage effectively. Furthermore, the expression levels of DNA repair-related proteins phospho-ataxia telangiectasia mutated (phospho-ATM) and phospho-ataxia telangiectasia mutated and Rad3-related (phospho-ATR) in cells pretreated with fisetin micelles were obviously lower than those in radiotherapy alone group (Fig. 2G). Correspondingly, the repair capacity of DNA double-strand breaks de-

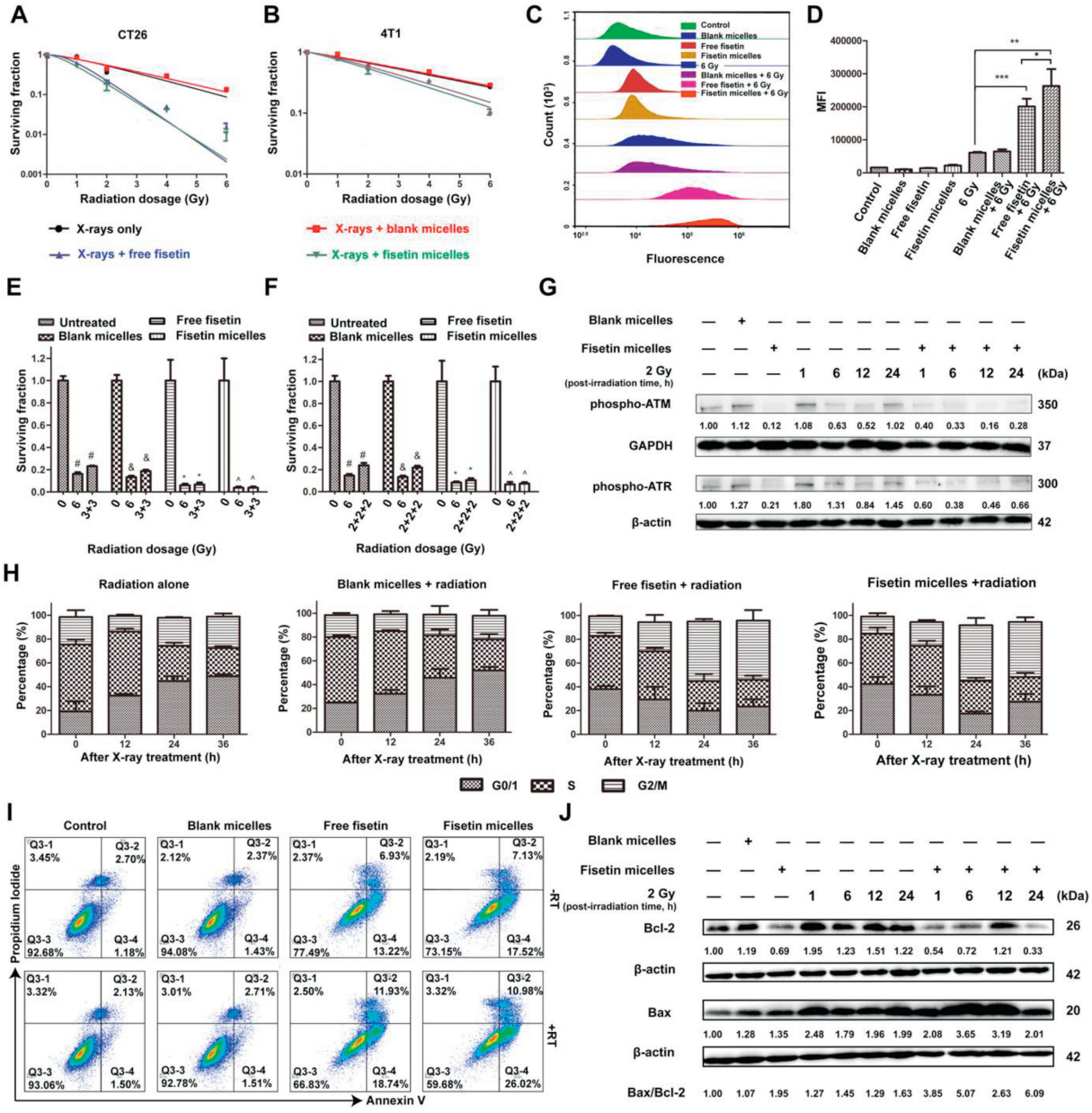

Fig. 2. Radiosensitization effect of fisetin micelles *in vitro*. Cell survival curves were determined by colony formation method in CT26 cells (A) and 4T1 cells (B); flow cytometric histograms (C) and mean fluorescence intensity (MFI, D) of ROS accumulated in CT26 cells. $^{*}P < 0.05$, $^{**}P < 0.01$, $^{***}P < 0.001$. (E) Cell surviving fractions after single (6 Gy) and split doses of radiation (3/3 Gy). #, recovery ratio = 1.43; &, recovery ratio = 1.40; *, recovery ratio = 1.11; ^, recovery ratio = 1.00. (F) Cell surviving fractions after single (6 Gy) and split doses of radiation (2/2/2 Gy). #, recovery ratio = 1.62; &, recovery ratio = 1.64; *, recovery ratio = 1.25; ^, recovery ratio = 1.11. (G) Levels of phospho-ATM and phospho-ATR were ascertained by Western blot in CT26 cells. (H) Cell cycle distribution after different treatment. (I) Effects of fisetin micelles pretreatment on apoptosis in CT26 cells. (J) Levels of Bcl-2 and Bax were ascertained by Western blot analysis in CT26 cells. Data are presented as the means ± SD ($n = 3$). GAPDH: glyceraldehyde-3-phosphate dehydrogenase.

creased in the fisetin micelles combined with radiotherapy group. It is well-established that normal tissues have a more robust capability to repair DNA damage than malignant tissues. Although the difference is not apparent after a single conventional dose irradiation of 2 Gy, the difference is exponentially amplified after dozens of irradiations. The gap in the ability to repair DNA damage between normal tissues and tumor tissues will be further enlarged when fisetin micelles are combined with radiotherapy, creating the possibility of complication-free tumor control.

Cell cycle distribution and apoptosis analysis were further performed to evaluate fisetin micelles-mediated radiosensitization in tumor cells. As displayed in Fig. S6 (Supporting information) and Fig. 2H, cells in radiation alone and blank micelles combined with radiotherapy groups were blocked in G0/G1 phase of the cell cycle, accompanied by a decrease of cell proportion in S phase after irradiation. For cells pretreated with fisetin micelles, the percentage of cells in G2/M phase increased by 31.87%, whereas that in S phase decreased by 21.42% after radiotherapy followed by a post-irradiation period of 36 h. The results showed that cells pretreated with fisetin micelles were blocked in a more radiosensitive cell cycle phase (G2/M phase) after radiotherapy, and the radiosensitivity of the cells was accordingly improved. More importantly, the apoptosis rate of the fisetin micelles combined with radiotherapy group was significantly higher than that of the radiotherapy alone group or the fisetin micelles group (Fig. 2I and Fig. S7 in Supporting information). Expression levels of apoptotic-related proteins Bcl-2

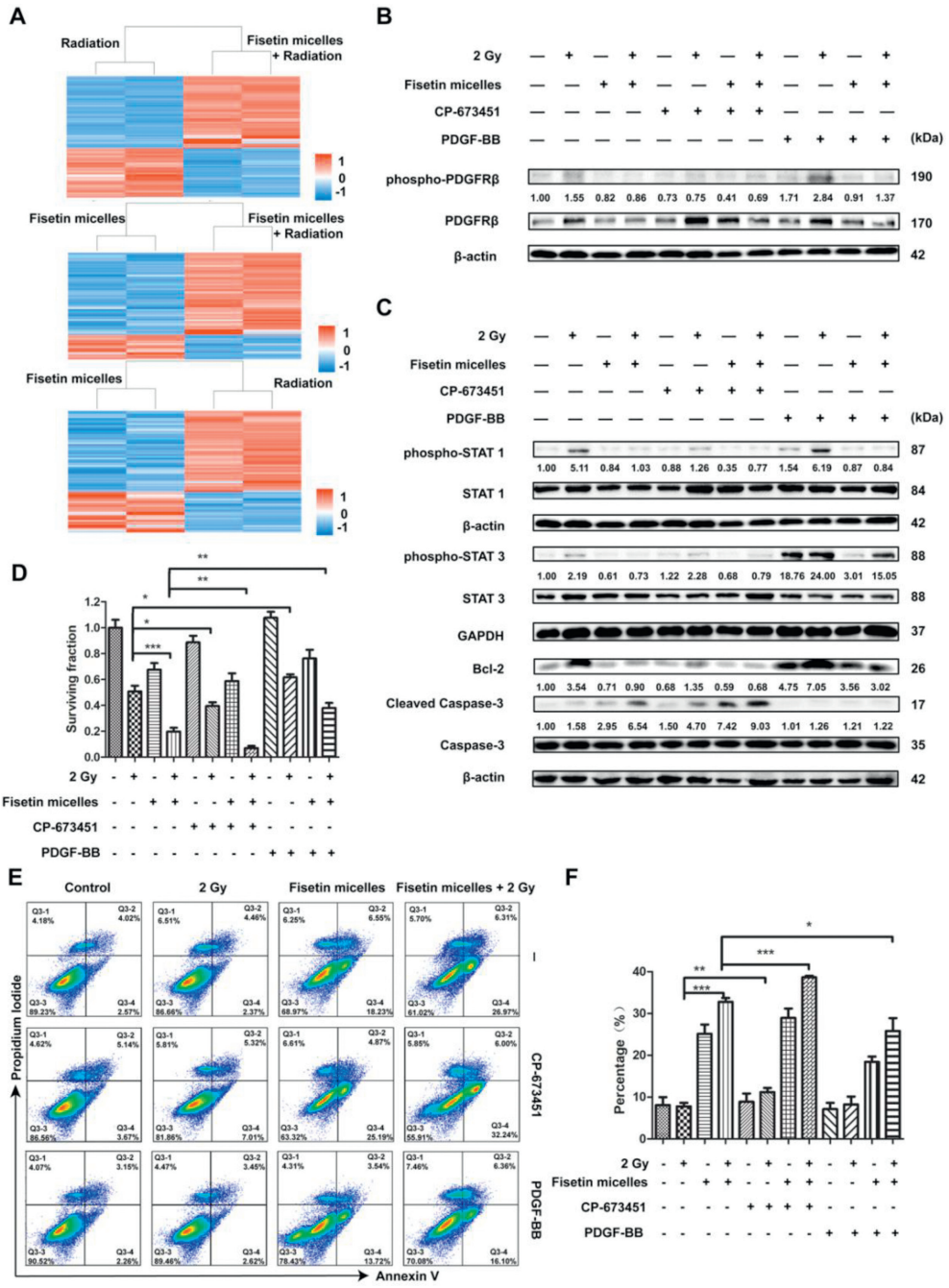

Fig. 3. Fisetin micelles inhibited the activation of PDGFRβ/STAT1/STAT3/Bcl-2 pathway after irradiation to promote tumor cell death. (A) Clustering analysis results of the DEPs. (B) Fisetin micelles inhibited the expression and activation of PDGFRβ after radiotherapy. (C) Fisetin micelles inhibited PDGFRβ/STAT1/STAT3/Bcl-2 pathway activity after radiotherapy. (D) Cell surviving fractions were determined by colony formation method to evaluate the modification of radiation effect by fisetin micelles, CP-673451 and PDGF-BB in CT26 cells. (E) Effects of fisetin micelles, CP-673451 and PDGF-BB pretreatment on radiation-induced apoptosis in CT26 cells. (F) The percentage of apoptotic cells under different pretreatments. Data are presented as the means ± SD ($n = 3$). $^{*}P < 0.05$, $^{**}P < 0.01$, $^{***}P < 0.001$.

and Bcl-2 associated X (Bax) were also ascertained. As indicated in Fig. 2J, fisetin micelles significantly up-regulated the Bax/Bcl-2 expression ratio after radiotherapy and induced cell apoptosis, which was consistent with findings by flow cytometry (FCM). All these promising results indicated that the safe and soluble radiosensitizer fisetin micelles possessed excellent potential for enhancing the radiosensitization effect and exhibited superior therapeutic efficiency *in vitro*.

To identify the molecular mechanisms involved in fisetin micelles radiosensitization, proteomic analysis was performed to determine which proteins were differentially expressed. A total of 396 differentially expressed proteins (DEPs) (264+/132-) were screened between the radiation and fisetin micelles group, 454 DEPs (184+/270-) between the radiation and combination treatment group, and 429 DEPs (136+/293-) between the fisetin micelles and combination treatment group. As shown in Fig. 3A, clustering analysis results of the DEPs demonstrated that the data patterns were highly similar within a group and relatively dissimilar between groups, and the DEPs' consistency was well. Gene ontology (GO) and Kyoto encyclopedia of genes and genomes (KEGG) enrichment analyses were performed on the DEPs, and the results were displayed in Figs. S8–S13 (Supporting information). Further-

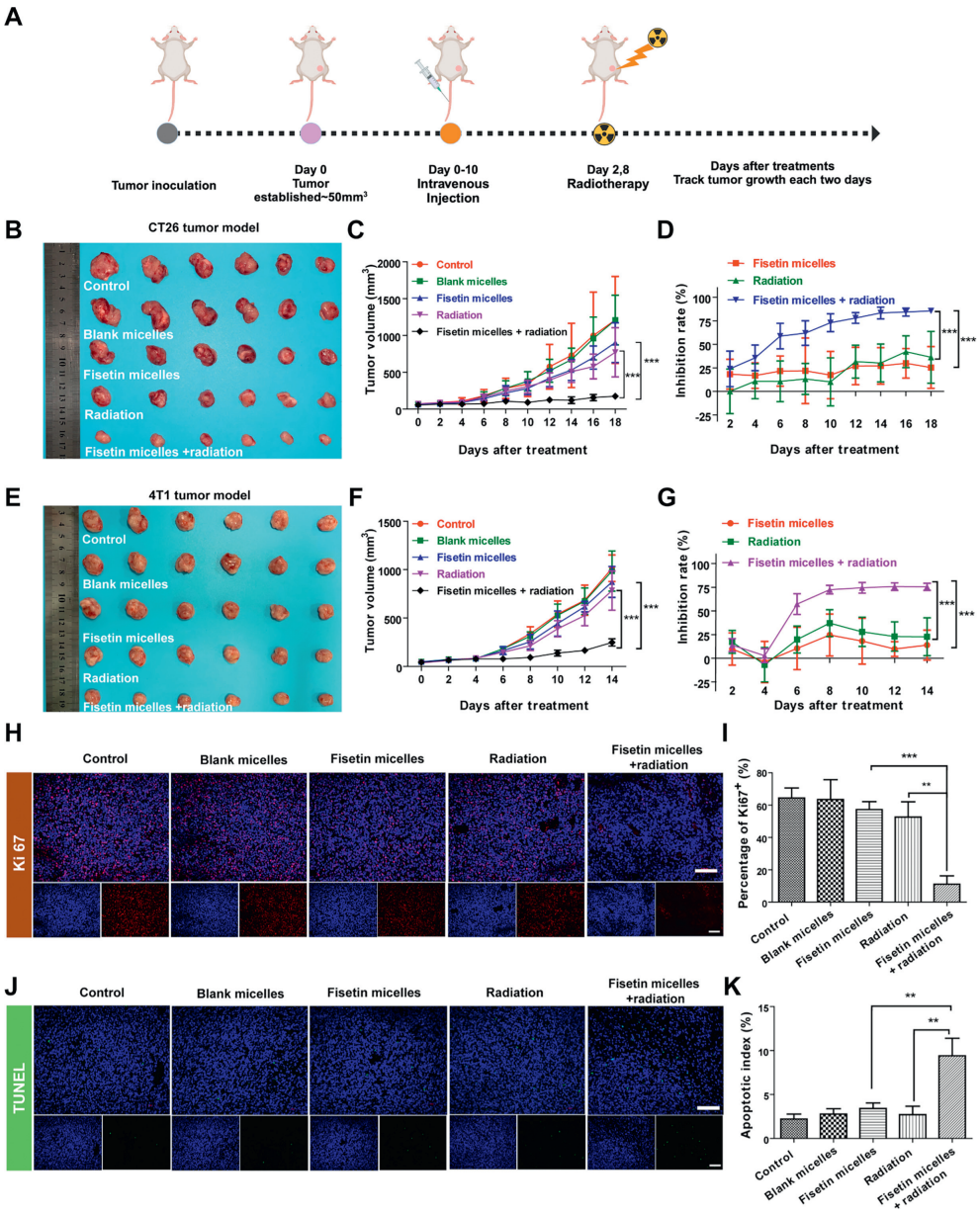

Fig. 4. Radiosensitization effect of fisetin micelles *in vivo*. (A) Schematic illustration of experimental design *in vivo*. The image (B) and tumor growth curves (C) of the tumors in CT26 tumor model; Inhibition rates based on tumor volume (D) in subcutaneous CT26 tumor model ($n = 6$). The image (E) and tumor growth curves (F) for each group in the 4T1 tumor model. Inhibition rates based on tumor volume (G) in subcutaneous 4T1 tumor model ($n = 6$). Representative Ki67 (H, I) and TUNEL (J, K) immunofluorescent staining results of tumor tissues in subcutaneous CT26 tumor mode ($n = 3$). Scale bar: 100 μm. Data are presented as the means ± SD. $^{**}P < 0.01$, $^{***}P < 0.001$.

more, protein-protein interactions were constructed (Figs. S14–S16 in Supporting information). We noticed that PDGFRβ was situated at a critical node of the interaction network of DEPs between the radiotherapy and the combination treatment group. According to the quantification analysis, the expression level of PDGFRβ in the combination treatment group was significantly lower than that in radiotherapy group ($P < 0.001$). Previous studies have shown that inhibition of PDGFRβ expression helped enhance tumor radiosensitivity [32,33]. Consequently, we speculated that fisetin micelles radiosensitization was related to altered expression level of PDGFRβ.

To clarify the role of PDGFRβ in fisetin micelles radiosensitization, the modification of radiation effect and influences on related protein expression by CP-673451 (a selective PDGFRβ inhibitor) and platelet-derived growth factor-BB (PDGF-BB, a PDGFRβ ligand) were further evaluated, using FCM, Western blot assay and colony-forming experiment. The results of Western blot assay (Fig. 3B), in agreement with the proteomics technology results, demonstrated that fisetin micelles could significantly down-regulate PDGFRβ expression after irradiation. In addition, PDGFRβ was activated after radiotherapy. The activation of PDGFRβ involves multiple downstream signaling pathways, among which Janus kinase (JAK)/STAT pathway was reported to be related to the radioresistance of various malignant tumors [34,35]. Western blot assays revealed that PDGFRβ/STAT1/STAT3/Bcl-2 signal pathway was activated after irradiation, whereas fisetin micelles suppressed this pathway activity (Fig. 3C). Besides, the results indicated that CP-673451 could intensify the inhibitory effect of fisetin micelles on PDGFRβ/STAT1/Bcl-2 pathway activity, while PDGF-BB could weaken the inhibitory effect of fisetin micelles on PDGFRβ/STAT3/Bcl-2 pathway activity after radiotherapy. Further, cell surviving fractions and apoptosis rates were determined to evaluate the modification of radiation effect by fisetin micelles, CP-673451 and PDGF-BB. As shown in Fig.

3D, cell surviving fraction was significantly decreased after fisetin micelles ($P < 0.001$) or CP-673451 pretreatment ($P < 0.05$), but increased after PDGF-BB pretreatment ($P < 0.05$). What was more, as compared with fisetin micelles pretreatment, the survival fraction at 2 Gy was obviously decreased after fisetin micelles and CP-673451 coadministration ($P < 0.01$) and increased after fisetin micelles and PDGF-BB coadministration ($P < 0.01$). Regarding the effects of fisetin micelles, CP-673451 and PDGF-BB pretreatment on radiation-induced apoptosis, the apoptosis rates under different pretreatments were exhibited in Figs. 3E and F. Compared with the combination of fisetin micelles with radiation, the combined treatment of fisetin micelles and CP-673451 with radiotherapy dramatically increased apoptosis rate ($P < 0.001$). However, the apoptosis rate of the fisetin micelles and PDGF-BB combined with radiotherapy group was lower than that of the fisetin micelles combined with radiotherapy group ($P < 0.05$). These findings were also consistent with the expression levels of cleaved caspase-3 in each group (Fig. 3C). The above results suggested that CP-673451 promoted cell death after radiotherapy and enhanced the radiosensitization effect of fisetin micelles, while the opposite role of PDGF-BB. Specifically, PDGFRβ/STAT1/STAT3/Bcl-2 pathway was activated and promoted tumor cell survival after radiotherapy, and fisetin micelles played a role in radiotherapy sensitization by suppressing this pathway.

To evaluate whether the radiosensitization effect observed *in vitro* could be translated into therapeutic efficacy *in vivo*, mouse models of colon and breast cancer were developed. Animal studies were performed in accordance with the protocol provided by the Institutional Animal Care and Use Committee of Sichuan University. In the two models, mice of the radiotherapy and combined treatment groups were irradiated with 2 Gy X-rays after tail vein administration on days 2 and 8 (Fig. 4A). Although fisetin micelles or radiotherapy alone could inhibit tumor growth to varying degrees, fisetin micelles combined with radiotherapy groups obtained the strongest suppression of tumor growth both in the CT26 (Figs. 4B–D and Fig. S17 in Supporting information) and 4T1 tumor models (Figs. 4E–G and Fig. S18 in Supporting information). The tumor inhibition rates based on tumor weight and tumor volume further supported these results (Tables S3 and S4 in Supporting information), indicating a synergy between fisetin micelles and radiotherapy to inhibit cancer growth. Besides, EF values were calculated to evaluate the radiosensitization effect based on tumors to grow to 3 and 6 times the original volume (TGT3 and TGT6). As shown in Tables S5 and S6 (Supporting information), EFs for CT26 tumor were 5.02 and 5.38, while for 4T1 tumor were 4.58 and 4.8, according to TGT3 and TGT6, respectively. CT26 tumor model responded better than 4T1 tumor model when combining fisetin micelles with radiation, consistent with the above *in vitro* study.

These findings underscored the potential of fisetin micelles as a promising radiosensitizer applicable to various types of tumor cells. Meanwhile, to further verify the superior therapeutic efficacy *in vivo*, necrosis, cell proliferation, and apoptosis of CT26 tumor were performed by hematoxylin-eosin (H&E), Ki67, and transferase-mediated nick-end labeling (TUNEL) labeling staining. Consistent with the observed results of tumor suppression, fisetin micelles combined with radiotherapy aggravated tumor cell necrosis (Fig. S19 in Supporting information) and exhibited the lowest proliferation (Figs. 4H and I), along with the highest apoptosis (Figs. 4J and K). Furthermore, treatment with the combination of fisetin micelles and radiation caused no apparent weight loss (Fig. S20 in Supporting information) and no abnormal changes in blood routine and serum biochemistry (Figs. S21–S24 in Supporting information) in CT26 and 4T1 tumor models. Additionally, there was no observed toxicity to the susceptible organs of mouse (Fig. S25 in Supporting information). Taking the above results, the combination of fisetin micelles and radiotherapy treatment exhibited better antitumor efficiency with no noticeable toxic effects on mice and possessed potential as a powerful radiosensitizer for clinical application.

In summary, this study designed a safe and soluble radiosensitizer fisetin micelles to precisely exhibit a significant radiosensitization effect both *in vitro* and *in vivo*. A novel observation of this study was that fisetin micelles could inhibit the activation of PDGFRβ/STAT1/STAT3/Bcl-2 pathway after radiotherapy to promote malignant cell death. Moreover, using SER and EF values to quantify its radiosensitizing effect, we provided evidence that fisetin micelles were cell-selective, and that the enhancement of normal tissue cells was much less than for any of the tumors studied. Collectively, fisetin micelles, through inhibiting a specific signaling pathway, exhibit potential as a low-toxic and highly effective radiosensitizer for tumor therapy, providing the theoretical and experimental basis to narrow the current gap in the translation of these nanotechnologies to the clinic.

Declaration of competing interest

The authors declare that they have no known competing financial interests or personal relationships that could have appeared to influence the work reported in this paper.

Acknowledgments

This work was funded by a grant from Technology Project of Science and technology department of Sichuan province (No. 2018SZ0021). Graphical abstract and schematic illustration of experimental design *in vivo* (Fig. 4A) was created with BioRender.com, and we would like to express our gratitude to BioRender.com for the drawing material.

Supplementary materials

Supplementary material associated with this article can be found, in the online version, at doi:10.1016/j.cclet.2024.109734.

References

[1] R. Baskar, K.A. Lee, R. Yeo, K.W. Yeoh, Int. J. Med. Sci. 9 (2012) 193–199.
[2] L. Wen, L. Chen, S. Zheng, et al., Adv. Mater. 28 (2016) 5072–5079.
[3] P. Dent, A. Yacoub, J. Contessa, et al., Radiat. Res. 159 (2003) 283–300.
[4] H. Huang, Y.L. Feng, T. Wan, et al., JAMA Oncol. 7 (2021) 361–369.
[5] M. Miller, N. Hanna, BMJ 375 (2021) n2363.
[6] A.A. Forastiere, H. Goepfert, M. Maor, et al., N. Engl. J. Med. 349 (2003) 2091–2098.
[7] Y. Meng, S. Han, J. Yin, J. Wu, ACS Appl. Mater. Interfaces 15 (2023) 41743–41754.
[8] X. You, L. Wang, J. Zhang, et al., Chin. Chem. Lett. 34 (2023) 107720.
[9] J. Zhang, C. Wang, Y. Zhang, et al., Chin. Chem. Lett. 35 (2024) 109420.
[10] M.E. Werner, N.D. Cummings, M. Sethi, et al., Int. J. Radiat. Oncol. Biol. Phys. 86 (2013) 463–468.
[11] H. Hu, Z. Zhang, Y. Fang, et al., Chin. Chem. Lett. 34 (2023) 107953.
[12] Y. Tao, C. Dai, Z. Xie, et al., Chin. Chem. Lett. 35 (2024) 109170.
[13] N. Xu, J. Wang, L. Liu, C. Gong, Chin. Chem. Lett. 35 (2024) 109225.
[14] C. Ou, M. Xiao, X. Zheng, et al., Chin. Chem. Lett. 35 (2024) 109275.
[15] L.R.H. Gerken, M.E. Gerdes, M. Pruschy, I.K. Herrmann, Mater. Horiz. 10 (2023) 4059–4082.
[16] C. Li, X. You, X. Xu, et al., Adv. Sci. 9 (2022) e2104134.
[17] M.E. Werner, J.A. Copp, S. Karve, et al., ACS Nano 5 (2011) 8990–8998.
[18] J. Jung, S.J. Park, H.K. Chung, et al., Int. J. Radiat. Oncol. Biol. Phys. 84 (2012) e77–e83.
[19] X. Zhang, H. Yang, K. Gu, et al., Int. J. Nanomedicines 6 (2011) 437–444.
[20] C. Bilynsky, N. Millot, A.L. Papa, Bioeng. Transl. Med. 7 (2022) e10256.
[21] F. Boateng, W. Ngwa, Int. J. Mol. Sci. 21 (2019) 273.
[22] K.A. Mason, N.R. Hunter, U. Raju, et al., Int. J. Radiat. Oncol. Biol. Phys. 59 (2004) 1181–1189.
[23] U. Raju, E. Nakata, K.A. Mason, et al., Cancer Res. 63 (2003) 3263–3267.
[24] N. Watanabe, R. Hirayama, N. Kubota, J. Radiat. Res. 48 (2007) 45–50.
[25] N. Khan, M. Asim, F. Afaq, et al., Cancer Res. 68 (2008) 8555–8563.
[26] W.S. Chen, Y.J. Lee, Y.C. Yu, et al., Int. J. Radiat. Oncol. Biol. Phys. 77 (2010) 1527–1535.
[27] A. Pawar, S. Singh, S. Rajalakshmi, et al., Artif. Cells Nanomed. Biotechnol. 46 (2018) 347–361.

[28] L. Wei, C. Cai, J. Lin, T. Chen, Biomaterials 30 (2009) 2606–2613.
[29] H.I. Atiya, A. Dvorkin-Gheva, J. Hassell, et al., Anticancer Res. 39 (2019) 2277–2287.
[30] U.S. Srinivas, B.W.Q. Tan, B.A. Vellayappan, A.D. Jeyasekharan, Redox Biol 25 (2019) 101084.
[31] J.S. Bedford, Int. J. Radiat. Oncol. Biol. Phys. 21 (1991) 1457–1469.
[32] J.D. Hong, X. Wang, Y.P. Peng, et al., Oncol. Lett. 14 (2017) 329–336.
[33] X. Mu, J. Ma, Z. Zhang, et al., Int. J. Radiat. Biol. 91 (2015) 771–776.
[34] S.Y. Park, C.J. Lee, J.H. Choi, et al., J. Exp. Clin. Cancer Res. 38 (2019) 399.
[35] L. Lu, J. Dong, L. Wang, et al., Oncogene 37 (2018) 5292–5304.